Probing an Open CFTR Pore with Organic Anion Blockers

Zhen Zhou, Shenghui Hu, and Tzyh-Chang Hwang

Department of Physiology, Dalton Cardiovascular Research Center, University of Missouri-Columbia, Columbia, MO 65211

ABSTRACT The cystic fibrosis transmembrane conductance regulator (CFTR) is an ion channel that conducts Cl^- current. We explored the CFTR pore by studying voltage-dependent blockade of the channel by two organic anions: glibenclamide and isethionate. To simplify the kinetic analysis, a CFTR mutant, K1250A-CFTR, was used because this mutant channel, once opened, can remain open for minutes. Dose–response relationships of both blockers follow a simple Michaelis-Menten function with K_d values that differ by three orders of magnitude. Glibenclamide blocks CFTR from the intracellular side of the membrane with slow kinetics. Both the on and off rates of glibenclamide block are voltage dependent. Removing external Cl^- increases affinity of glibenclamide due to a decrease of the off rate and an increase of the on rate, suggesting the presence of a Cl^- binding site external to the glibenclamide binding site. Isethionate blocks the channel from the cytoplasmic side with fast kinetics, but has no measurable effect when applied extracellularly. Increasing the internal Cl^- concentration reduces isethionate block without affecting its voltage dependence, suggesting that Cl^- and isethionate compete for a binding site in the pore. The voltage dependence and external Cl^- concentration dependence of isethionate block are nearly identical to those of glibenclamide block, suggesting that these two blockers may bind to a common binding site, an idea further supported by kinetic studies of blocking with glibenclamide/isethionate mixtures. By comparing the physical and chemical natures of these two blockers, we propose that CFTR channel has an asymmetric pore with a wide internal entrance and a deeply embedded blocker binding site where local charges as well as hydrophobic components determine the affinity of the blockers.

KEY WORDS: chloride channel • voltage-dependent block • multi-ion pore • ion permeation

INTRODUCTION

Cystic fibrosis transmembrane conductance regulator (CFTR)* is an ion channel that conducts Cl^- ions (for review see Sheppard and Welsh, 1999). Malfunction of CFTR, due to mutations of the gene coding for CFTR, results in cystic fibrosis (Riordan et al., 1989). It is suggested, from hydropathy studies, that CFTR consists of two membrane-spanning domains, each of which contains six transmembrane segments that are thought to form the anion-selective pore. In addition to these two membrane-spanning domains, there are two nucleotide-binding domains (NBD1 and NBD2) that presumably carry out the ATP hydrolysis reaction that gates the channel, and a regulatory domain (R domain), phosphorylation of which regulates channel activity (for review see Gadsby et al., 1995).

Despite numerous physiological and biophysical studies of CFTR functions, the structure of CFTR remains undefined due to a lack of crystal structure. However, previous investigations using mutagenesis suggest that the sixth transmembrane segment (TM6) may play an important role in forming the pore (Tabcharani et al., 1993; Akabas et al., 1994; Mansoura et al., 1998). Other transmembrane segments, such as TM5 (Mansoura et al., 1998) and TM12 (McCarty et al., 1993; McDonough et al., 1994) may also contribute to the pore formation. Since large organic anions (e.g., DIDS, DNDS, glutamate, and gluconate) can only block the channel when applied internally, it is proposed that the CFTR pore is asymmetric with a relatively large internal vestibule to accommodate those sizable blockers (Linsdell and Hanrahan, 1996a,b; Linsdell et al., 1997). However, a symmetric pore model has been successfully used to explain the selectivity mechanism among lyotropic anions (Smith et al., 1999).

Several lines of evidence suggest multi-ion occupancy of the CFTR pore. First, the anomalous mole fraction effect between Cl^- and thiocyanate (SCN^-), an indication of the existence of multi-ion binding sites, is observed in wild-type CFTR (wt-CFTR). Since this effect is abolished when the positive charge of Arg 347 (a residue in TM6) is neutralized, it is thought that Arg 347 forms one of the anion binding sites inside the pore (Tabcharani et al., 1993). Second, inhibition of the CFTR channel by internally applied blockers is affected by changing extracellular [Cl^-] (Linsdell et al., 1997; Sheppard and Robinson, 1997; Zhou et al., 2001b). Since the off rate of the blocker is increased by increasing extracellular [Cl^-], this trans-ion effect can be

Address correspondence to Tzyh-Chang Hwang, Dalton Cardiovascular Research Center, 134 Research Park, University of Missouri-Columbia, Columbia, MO 65211. Fax: (573) 884-4232; E-mail: hwangt@health.missouri.edu

*Abbreviations used in this paper: CFTR, cystic fibrosis transmembrane conductance regulator; NBD, nucleotide-binding domain.

explained by an electrostatic repulsion between the blocker and the Cl^- ion simultaneously present in the pore (e.g., Zhou et al., 2001b). However, it is also possible that external Cl^- and internally applied blocker may compete for a common binding site (e.g., Sheppard and Robinson, 1997). This latter scenario would predict that the on rate of the blocker is decreased by increasing extracellular [Cl^-]. Thus, to distinguish these two mechanisms, it is essential to investigate how external [Cl^-] affects the association and dissociation rates of the blocker with single-channel kinetic analysis. Third, models with two or three binding sites have been used successfully to describe gluconate and SCN^- block of the CFTR channel (Linsdell et al., 1997). Recently, a model with three binding sites is used to explain the role of Arg 334, a charged residue in TM6, in conduction properties (Smith et al., 2001). However, the multi-ion pore notion has been challenged by some other reports. First, Cotton and Welsh (1999) conclude that instead of forming an anion binding site directly, Arg 347 may form a salt bridge with Asp 924 to stabilize the channel architecture. Second, the anomalous mole fraction effect described above is not observed in some studies (Mansoura et al., 1998). In addition, a higher single-channel conductance with SCN^- as the charge carrier, observed in earlier experiments demonstrating the anomalous mole fraction effect (Tabcharani et al., 1993), is recently challenged (Linsdell, 2001). Third, a single-ion pore model is shown to adequately explain the anion selectivity of CFTR (Smith et al., 1999).

The goal of the current study is to probe the CFTR channel with organic anion blockers to gain some insight into the structural properties of the anion-conducting pore. High affinity blockers have been proven to be invaluable tools in elucidating the pore structure of ion channels. The most successful examples are the well-known potassium channel blockers: TEA and its derivatives (e.g., Armstrong, 1971; Miller, 1982; Choi et al., 1993). Importantly, early biophysical work using blockers to probe the properties of the ion binding sites in the potassium channel pore is supported by recent x-ray crystallographic studies of the KcsA potassium channel (Doyle et al., 1998; Jiang and MacKinnon, 2000; Zhou et al., 2001a). In this study, two organic anion blockers, glibenclamide and isethionate, were used to probe the CFTR pore. Glibenclamide, the most potent CFTR blocker found so far, is an anion with large hydrophobic components (Schultz et al., 1996; Sheppard and Robinson, 1997; Gupta and Linsdell, 2002). Here, mechanisms underlying the voltage-dependent blockade by glibenclamide were studied in detail using single-channel and whole-cell recordings. On the other hand, isethionate is an anion that has been used widely as a Cl^- substitute. Our results indicate that isethionate effectively blocks CFTR and is more potent than some of the known hydrophilic anion blockers, such as gluconate and glutamate (Linsdell and Hanrahan, 1996b; Linsdell et al., 1997). It blocks the channel from the cytoplasmic side of the membrane with a voltage dependence that is nearly identical to that of glibenclamide. In addition, removing external Cl^- has virtually identical effects on isethionate and glibenclamide blockage. Furthermore, results obtained from experiments using mixtures of glibenclamide and isethionate are consistent with a model that two blockers compete for a common binding site. Structural implications of the CFTR pore based on the comparison of physical and chemical natures of glibenclamide and isethionate are discussed.

MATERIALS AND METHODS

Cell Preparation

NIH3T3 cells stably expressing K1250A-CFTR channels (Zeltwanger et al., 1999) were maintained at 37°C and 5% CO_2 in Dulbecco's Modified Eagle's Medium (DMEM) supplemented with 10% fetal bovine serum. Cells were passed twice a week in 25-cm^2 cell culture flasks. 2–5 d before patch-clamp recordings, cells were plated on small, sterile glass coverslips in 35-mm tissue culture dishes.

Single-channel Patch-clamp Recordings

Recording pipette electrodes were prepared with a two-stage vertical puller (Narishige) and were then fire polished using a homemade microforge to yield a pipette resistance of 3–6 MΩ when filled with the standard pipette solution. Right before the recording, a glass coverslip with cells grown on was placed into a continuously perfused chamber on the stage of an inverted microscope (Olympus). The standard pipette (external) solution (154 mM [Cl^-]o) contained (in mM): 140 NMDG-Cl, 2 $MgCl_2$, 5 $CaCl_2$, and 10 Hepes (pH 7.4 with NMDG). In some experiments, a pipette solution (0 Cl^- pipette solution) that contained (in mM) 154 NMDG-aspartate, 2 $MgSO_4$, and 10 HEPES (pH 7.4 with NMDG) was used to remove Cl^- in the external solution. For these experiments, recording pipettes were first filled with the 0 Cl^- pipette solution and a 6 mM Cl^- pipette solution was added onto the top portion of the pipette solution. The 6 mM Cl^- pipette solution contained (in mM): 148 aspartate, 2 $MgCl_2$, 1 $CaCl_2$, and 10 HEPES (pH 7.4 with NMDG). Cells were perfused with a bath solution containing (in mM): 145 NaCl, 5 KCl, 2 $MgCl_2$, 1 $CaCl_2$, 5 glucose, 5 Hepes, and 20 sucrose (pH 7.4 with NaOH). After the establishment of an inside-out configuration, the patch was perfused with a standard internal perfusion solution (154 mM [Cl^-]i) containing (in mM): 150 NMDG-Cl, 2 $MgCl_2$, 10 EGTA, and 8 Tris (pH 7.4 with NMDG). For Cl^- competition experiments, an internal perfusion solution containing (in mM): 296 NMDG-Cl, 2 $MgCl_2$, 10 EGTA, and 8 Tris (pH 7.4 with NMDG) was used.

Single-channel currents were recorded at room temperature (~22°C) using an EPC9 patch-clamp amplifier (Heka Electronic). Current traces were filtered at 100 Hz with a built-in 4-pole Bessel filter and stored on videotapes. Stationary current recordings were played back without further filtering, digitized at 500 Hz, and stored on the hard disk. To quantify fast blockade by isethionate, currents in response to 1 s voltage ramp ranging from −120 to 120 mV were recorded, filtered at 100 Hz with a built-in 4-pole Bessel filter, and digitized online at 2 kHz.

Whole-cell Patch-clamp Recordings

Whole-cell recordings were made using an EPC9 patch-clamp amplifier. The standard pipette (internal) solution contained (in mM): 101 CsCl, 2 $MgCl_2$, 20 TEACl, 10 MgATP, 8 Tris, 10 EGTA, and 5.8 glucose (pH 7.4 with CsOH). The standard bath (external) solution contained (in mM): 114 NaCl, 2 $MgCl_2$, 1 $CaCl_2$, 5 KCl, 5 Hepes, 5 glucose, and 70 sucrose (pH 7.4 with NaOH). In those experiments studying external isethionate block, the bath solution with isethionate contained (in mM): 76 isethionate, 75 NaCl, 5 KCl, 5 glucose, 5 Hepes, 2 $MgCl_2$, and 1 $CaCl_2$. The control bath solution contained (in mM): 152 sucrose, 75 NaCl, 5 KCl, 5 glucose, 5 Hepes, 2 $MgCl_2$, and 1 $CaCl_2$. 10 μM forskolin was used to activate the channel activity. Pulse and PulseFit program (Heka Electronic) was used to generate the voltage step protocol and collect the data. Cells were held at 0 mV before the voltage was stepped to various potentials from −120 to 120 mV for 500 ms in 20-mV increments, and then back to 0 mV. Current responses were filtered at 5 kHz and digitized online at 10 kHz. Steady-state currents were measured as the average current value of final 50 ms of the voltage step.

Data Analysis

For quantitative analysis of glibenclamide blockade, channel open probability (Po) was estimated from all-point amplitude histograms using the PAT program (Version 7.0, Strathclyde Electrophysiology Software). Single-channel kinetic analysis was performed using the software written by Dr. Csanády (Csanády, 2000). This program allows extraction of individual rate constants, given a kinetic model. All curve fittings were performed with Igor Pro program (Version 3.11, Wavemetrics) using a Levenberg-Marquardt algorithm. For quantitative analysis of isethionate blockade, net K1250A-CFTR single-channel I-V relationships were obtained by subtracting the I-V relationship of the leak (i.e., basal conductance before the channel is opened) from that of a single locked-open K1250A-CFTR channel. Usually, several voltage ramps were applied during a single opening to generate the I-V relationships. The average of these I-V relationships were then calculated to represent the single-channel I-V curve of K1250A-CFTR. Because of the small conductance of the CFTR channel and the extra noise introduced by the blocker, the signal-to-noise ratio is often jeopardized even when the current is filtered at 100 Hz. Therefore, we fit the averaged single-channel I-V curve with a four term polynomial function (fitted I-V). Fraction of block (Fb) was calculated according to the equation:

$$Fb = 1 - (I_b)/(I_o),$$

where I_b and I_o represent the fitted values of the block and unblocked current, respectively. Since Fb of isethionate was obtained in an open channel without interference of fast flickery block, a simple two state scheme (i.e., open ↔ blocked) was used for data analysis. Dissociation constant (K_d) for isethionate block can then be calculated according to Gupta and Linsdell (2002):

$$K_d = (1 - Fb)[Isethionate]/Fb. \quad (1)$$

To calculate K_d for glibenclamide block from single-channel data, a three state kinetic scheme (i.e., blocked ↔ open ↔ blocked) was used since the presence of fast flickery block in single-channel recordings has to be taken into account (see RESULTS for details). The relationship between K_d and Fb was described by Sheppard and Robinson (1997) as:

$$K_d = (1 - Fb)P_{oc}[Glibenclamide]/Fb, \quad (2)$$

where P_{oc} represents the open probability in the absence of the blocker.

Voltage dependence of the on rate ($k_{on}[V]$) and off rate ($k_{off}[V]$) of the blocker was estimated using Eqs. 3 and 4 according to the rate theory:

$$k_{on}(V) = k_{on}(V)'[X] = k_{on}(0)'[X]\exp(z\delta_{on}FV/RT) \quad (3)$$

$$k_{off}(V) = k_{off}(V)\exp(-z\delta_{off}FV/RT), \quad (4)$$

where $k_{on}(V)'$ is the second-order rate constant for blocker binding, $k_{on}(0)'$ is the second-order rate constant for blocker binding at 0 mV, $k_{off}(0)$ is the off rate of the blocker at 0 mV, [X] is the concentration of the blocker, δ_{on} is the electrical distance of the entry barrier, δ_{off} is the electrical distance of the exit barrier (δ_{on} and δ_{off} have values between 0 and 1), z is the valence of the blocker (a value of −1 is assumed for glibenclamide and isethionate), and F, R, and T have their usual thermodynamic meanings. Voltage dependence of K_d ($K_d[V]$) was estimated according to the following equation:

$$\begin{aligned} K_d(V) &= k_{off}(V)/k_{on}(V)' \quad (5)\\ &= k_{off}(0)/k_{on}(0)'\exp(-z[\delta_{on} + \delta_{off}]FV/RT)\\ &= K_d(0)\exp(-z\delta_{K_d}FV/RT), \end{aligned}$$

where $K_d(0)$ is the dissociation constant of the blocker at 0 mV; δ_{Kd} is the sum of δ_{on} and δ_{off} and represents the electrical distance of the blocker binding site from the inside of the channel.

All averaged data are expressed as means ± SEM; *n* represents the number of patches. Student *t* tests were performed using SigmaPlot (version 4.0) and effects were considered significant if $P < 0.05$.

RESULTS

Glibenclamide Block of K1250A-CFTR Channels

Previous studies show that glibenclamide blocks CFTR channels with a time constant in the range of tens of milliseconds that is slow enough to be resolved in single-channel recordings (Schultz et al., 1996; Sheppard and Robinson, 1997). However, this time constant of glibenclamide block is very close to the closed time constant of ATP-gated events in wt-CFTR (Zeltwanger et al., 1999). Thus, unless ATP-dependent gating is deliberately retarded, it is very difficult to dissect these two events kinetically. That glibenclamide may affect CFTR gating (Zeltwanger et al., 2000) further complicates the analysis and interpretation. To extract the kinetic parameters of glibenclamide-induced blocking events with minimal contamination of ATP-dependent gating events, we studied glibenclamide block with a CFTR mutant, K1250A-CFTR, instead of wt-CFTR. The advantage of using K1250A-CFTR is that this channel, once opened by ATP, can stay open for minutes even after a complete removal of ATP. By collecting data within a prolonged channel opening, we can study primarily glibenclamide-induced blocking events.

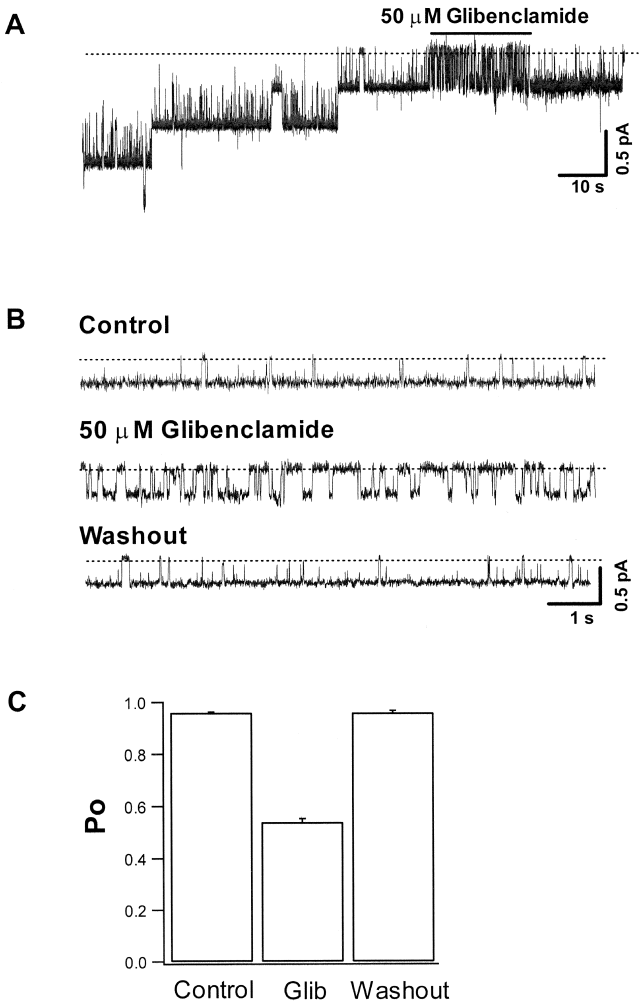

FIGURE 1. Glibenclamide block of K1250A-CFTR is reversible. K1250A-CFTR channel currents were activated by PKA and 1 mM ATP in an excised inside-out patch held at −50 mV with symmetric Cl^- (154 mM [Cl^-]o/154 mM [Cl^-]i). (A) Continuous recording of K1250A-CFTR after the channels were locked open with PKA and ATP. 50 μM glibenclamide, applied to the internal solution, exhibited its blocking effect within seconds. After washout of glibenclamide, single-channel current was reversed. (B) Expanded single-channel current traces before (Control), during and after (Washout) application of 50 μM glibenclamide. (C) Average Po from four patches before (Control), during (Glib), and after (Washout) the application of 50 μM glibenclamide. Dashed lines indicate the baseline level. Downward deflections represent channel openings.

We first tested whether glibenclamide block of K1250A-CFTR channels is similar to that of wt-CFTR channels. Fig. 1 A shows an example of glibenclamide-induced block recorded from an inside-out patch excised from an NIH3T3 cell stably expressing K1250A-CFTR. K1250A-CFTR currents were first activated by PKA and 1mM ATP (not depicted). In this particular example, at least three channels were activated and locked open. PKA and ATP were then removed and currents were allowed to relax. When there was only one channel left open, 50 μM glibenclamide was added to the superfusion solution. Glibenclamide-induced block was observed within seconds of the solution change (presumably limited by the speed of solution exchange). The block was readily reversed once the blocker was removed. Fig. 1 B shows expanded single-channel current traces before, during, and after glibenclamide application. Before application of glibenclamide, the channel stays in the locked-open state with occasional brief closings (i.e., flickery blocked state; see Zhou et al., 2001b). Glibenclamide (50 μM) induces frequent closed events that last for tens of milliseconds. In this particular experiment, open probability (Po) was reduced from 0.96 to 0.50 in the presence of 50 μM glibenclamide, and returned to 0.94 after glibenclamide was removed. There is no significant difference between the Po values before and after glibenclamide application (Fig. 1 C) (P = 1.0). Therefore, glibenclamide-induced block in K1250A-CFTR channels is completely reversible as seen in wt-CFTR (Schultz et al., 1996; Sheppard and Robinson, 1997; Gupta and Linsdell, 2002; cf. Sheppard and Welsh, 1992).

Next, we examined the sensitivity of K1250A-CFTR to glibenclamide block. Fig. 2 A shows representative single-channel current traces in the presence of various amounts of glibenclamide. As [glibenclamide] is increased, more blocked events are observed. Po before and during glibenclamide application was obtained from all-point amplitude histograms. Fraction of block (Fb) was calculated as $1 - Po_{w/\ glibenclamide}/Po_{w/o\ glibenclamide}$ (Fig. 2 B). The resulting dose–response relationship can be fitted with a Michaelis-Menten function with a $K_{1/2}$ of 49.4 ± 9.5 μM at −50 mV, which is similar to that reported for wt-CFTR (Schultz et al., 1996; Sheppard and Robinson, 1997), indicating that the K1250A mutation does not affect the sensitivity of the channel to glibenclamide.

We then tested whether glibenclamide blocks K1250A-CFTR channels in a voltage-dependent manner as shown for wt-CFTR channels (Sheppard and Robinson, 1997; Gupta and Linsdell, 2002). Fig. 3 A shows single-channel current traces at various membrane potentials in the presence of 50 μM glibenclamide. Po at each voltage was used to calculate Fb as described above. Fb increases with hyperpolarization as seen in wt-CFTR (Fig. 3 B, top). Using Eq. 2, we calculated K_d values at various voltages and the resulting data were fitted with Eq. 5 (Fig. 3 B, bottom), which yields a δ_{Kd} of 0.45 ± 0.03. This voltage dependence is similar to those reported previously for wt-CFTR (Sheppard and Robinson, 1997; Gupta and Linsdell, 2002). We therefore conclude that the mechanisms of voltage dependence of glibenclamide block for K1250A-CFTR channels can also be applied to wt-CFTR channels.

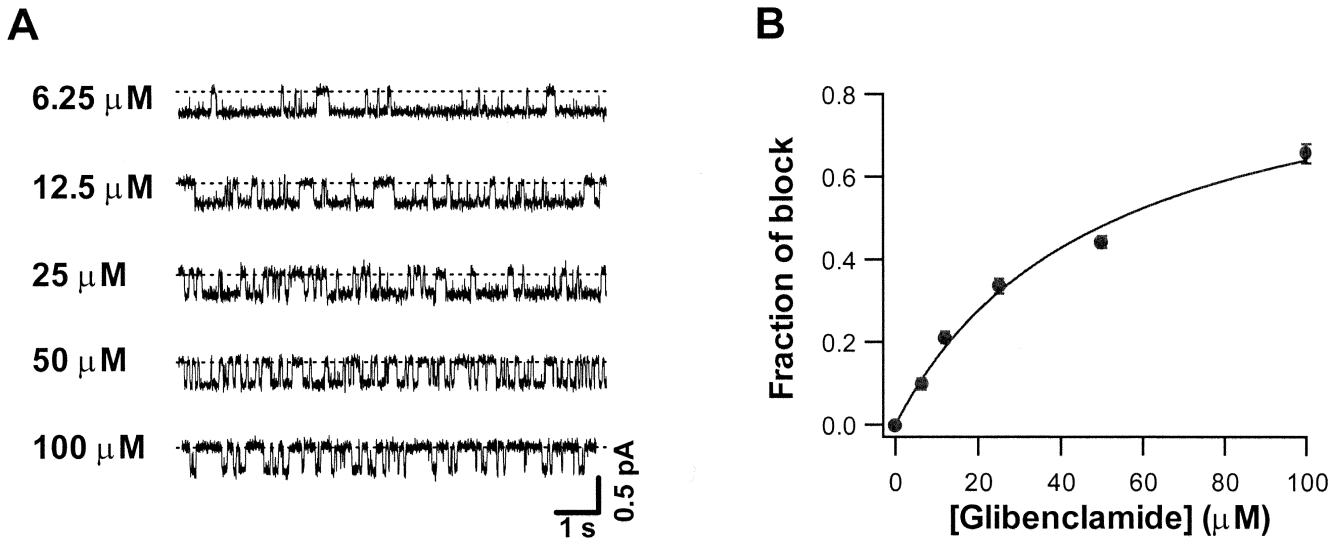

FIGURE 2. Dose–response relationship of glibenclamide block. (A) Single-channel current traces in the presence of various concentrations of glibenclamide. Inside-out patches were held at −50 mV under symmetric Cl^- condition (154 mM [Cl^-]o/154 mM [Cl^-]i). (B) Dose–response relationship of glibenclamide block. Each point represents the average from three to nine patches. Data are fitted with the Michaelis-Menten function (solid line): $Fb = Fb_{max}[X]/(K_{1/2} + [X])$, where Fb_{max} is the maximal fraction of block, [X] is the blocker concentration and $K_{1/2}$ is the concentration of blocker at which the fraction of block is half of the maximum.

Whole-cell Recordings of Glibenclamide Block of K1250A-CFTR

With single-channel recordings in excised inside-out patches, we were only able to investigate glibenclamide block at negative membrane potentials since patches became unstable when held at positive potentials for a long period of time (essential for kinetic analysis). To observe glibenclamide's blocking behavior over a broad voltage range, we switched to whole-cell patch-clamp recordings. After establishment of a whole-cell

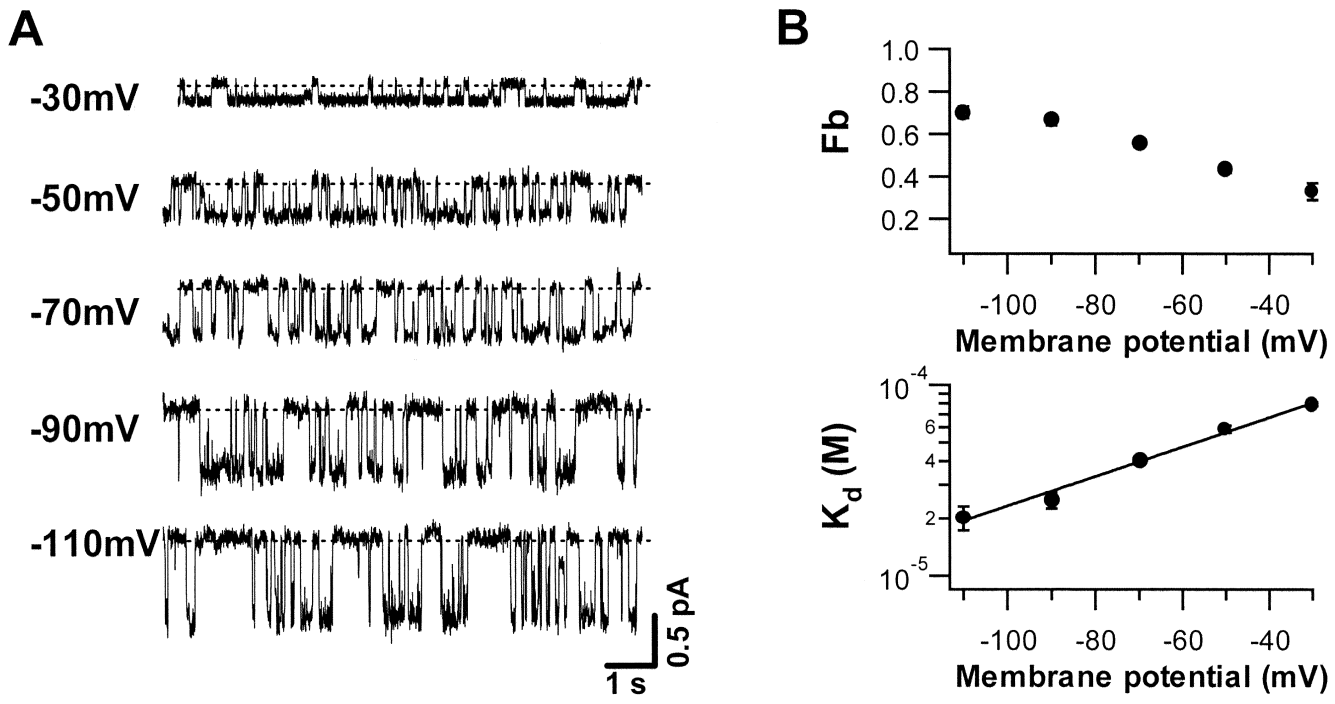

FIGURE 3. Voltage dependence of glibenclamide block. (A) Single-channel current traces in the presence of 50 μM glibenclamide at various membrane potentials. (B) Relationship between fraction of block (Fb), dissociation constant (K_d) and membrane potential. Fb was calculated from Po. K_d was calculated according to Eq. 2. Solid line denotes a fit of Eq. 5 to the results ($\delta_{Kd} = 0.45 \pm 0.03$). Each point represents the average from 3 to 13 patches.

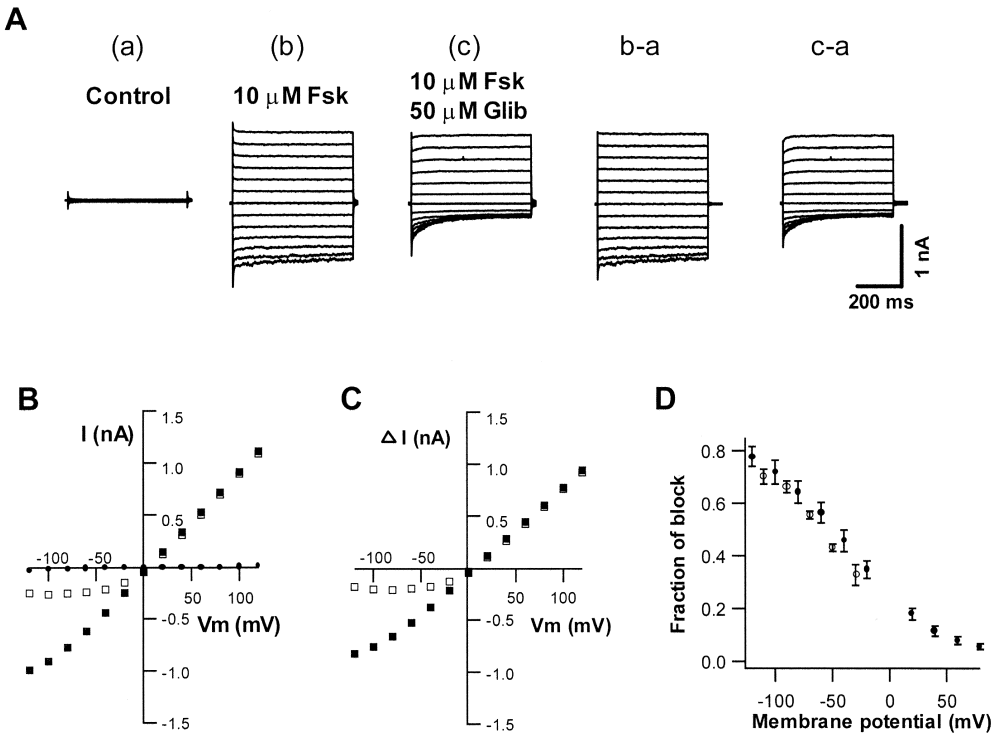

FIGURE 4. Glibenclamide block of whole-cell K1250A-CFTR currents. (A) Whole-cell currents in response to voltage steps from −120 to 120 mV for 500 ms in 20-mV increments under symmetric Cl^- condition (125 mM $[Cl^-]o$/125 mM $[Cl^-]i$). 10 μM forskolin (Fsk) or 10 μM Fsk/50 μM glibenclamide (Glib) was applied to the superfusion (external) solution. Net currents in the presence of 10 μM Fsk (b-a) or 10 μM Fsk/50 μM Glib (c-a) were obtained by subtracting the leak current (Control, a) from the current responses in the presence of 10 μM Fsk (b) or 10 μM Fsk/50 μM Glib (c). (B) Steady-state current-voltage (I-V) relationships of the leak (●), 10 μM Fsk (■), and 10 μM Fsk/50 μM Glib (□). (C) Net I-V relationships in the presence of 10 μM Fsk (■) and 10 μM Fsk/50 μM Glib (□). (D) Voltage dependence of glibenclamide block of K1250A-CFTR. Fraction of block in the presence of 50 μM glibenclamide (●) in whole-cell recordings was calculated from steady-state macroscopic currents. Fraction of block obtained from single-channel recordings (○; from Fig. 3 B) are superimposed.

configuration, 10 μM forskolin was applied to the bath solution to activate the channels. When whole-cell macroscopic currents reached a steady-state level, glibenclamide was added to the superfusion solution. It usually took several minutes for glibenclamide block to reach its steady-state. Fitting the time course of current inhibition with a single exponential function gave an average time constant of 76 ± 13 s (n = 3). This prolonged time course of glibenclamide block in the whole-cell configuration, contrary to the much faster block in inside-out patches (Fig. 1 A), is likely due to a slow permeation of glibenclamide through the cell membrane. Glibenclamide, although applied to the extracellular side of the channel, exerts its blocking effect from the intracellular side of the channel as proposed by others (Schultz et al., 1996; Sheppard and Robinson, 1997; Gupta and Linsdell, 2002). Supporting this notion, the dose–response relationship of glibenclamide block measured from whole-cell experiments yielded a similar $K_{1/2}$ as that from single-channel experiments in inside-out patches (unpublished data).

To study the voltage dependence of glibenclamide block in whole-cell configuration, we held the membrane potential at 0 mV and then stepped it to various voltages from −120 to 120 mV for 500 ms in 20-mV increments. Before the application of forskolin (Fig. 4 A, control), whole-cell basal (leak) conductance is minimal (whole-cell resistance = 3.9 GΩ for this particular cell), indicating very little basal CFTR channel activity. Once the forskolin-activated current reached a steady-state level, voltage steps were applied again. Net K1250A-CFTR current traces were obtained by subtracting the leak from the forskolin-activated current (Fig. 4 A). Note that the whole-cell current traces are mostly time independent except at very high negative membrane potentials where fast current relaxations are observed. These time-dependent currents at negative membrane potentials are caused by an intrinsic voltage-dependent flickery block that has been characterized previously (Zhou et al., 2001b; see below). In the presence of 50 μM glibenclamide, in addition to the fast relaxation component, a much slower current relaxation is observed together with a decrease of the steady-state current at hyperpolarizing voltages (Fig. 4, A and B). Net steady-state I-V relationships in the presence or absence of glibenclamide are shown in Fig. 4 C. Clearly, glibenclamide blocks whole-cell K1250A-CFTR currents in a voltage-dependent manner with more block at negative voltages. Fb was calculated from the steady-state currents and summarized results are shown in Fig. 4 D. The values of Fb obtained from single-channel recordings (from Fig. 3 B) are superimposed. The agreement between these two sets of data not only supports the notion that glibenclamide, even applied extracellularly, blocks CFTR channels from the cytoplasmic side, but also suggests that the voltage dependence of glibencla-

mide block measured over a limited voltage range in excised patches can be applied to a broader voltage range.

Kinetic Analysis of Voltage-dependent Block of Glibenclamide on K1250A-CFTR

For glibenclamide block of K1250A-CFTR, we were able to apply a simple scheme for kinetic analysis (Scheme I).

$$FB \underset{k_f}{\overset{k_{-f}}{\rightleftharpoons}} O \underset{k_{off}}{\overset{k_{on}}{\rightleftharpoons}} GB$$

SCHEME I

where O, GB, and FB represent the open state, glibenclamide-blocked state, and the intrinsic flickery block state, respectively. k_{on} is the apparent on rate of glibenclamide, which is the product of the second-order rate constant for glibenclamide binding (k_{on}') and [glibenclamide], and k_{off} is the off rate of glibenclamide. The parameters k_f and k_{-f} are the apparent on and off rate of the blockade by the intrinsic blocker, respectively. According to this scheme, the open time distribution will follow a single exponential function and the mean open time should be equal to $1/(k_{on} + k_f)$, whereas the closed time distribution will follow a double exponential function with one component (i.e., $1/k_{off}$) representing the glibenclamide-induced blocked events and the other ($1/k_{-f}$) representing the closed events induced by intrinsic flickery blockings. Previous studies suggest that the mean blocked time of glibenclamide is about an order of magnitude longer than that of the intrinsic blocker (Schultz et al., 1996; Sheppard and Robinson, 1997; Zhou et al., 2001b), therefore, we should be able to separate these two components readily.

Using the PAT analysis program, we constructed dwell-time histograms from the single-channel recordings in the presence of 12.5 or 50 μM glibenclamide (Fig. 5 A). As predicted, the open time histograms can be well fitted with a single exponential function (Fig. 5 A, solid curves) and the mean open time decreases with an increase of [glibenclamide]. Also consistent with Scheme I, the closed time histograms can be fitted with a double exponential function (Fig. 5 A, solid curves) with both time constants independent of [glibenclamide]. Furthermore, as predicted from Scheme I, the fraction of the second component increases as [glibenclamide] is increased. These observations justify the application of Scheme I in the data analysis. Individual rate constants for glibenclamide block were extracted with the software developed by Dr. Csanády (Csanády, 2000). Fig. 5 B shows the resulting on and off rates of glibenclamide block at various blocker concentrations. Consistent with the idea of a simple bimolecular reaction between glibenclamide and the channel (Scheme I), the on rate (k_{on}) increases linearly with [glibenclamide], whereas the off rate (k_{off}) is little affected by [glibenclamide]. The lines representing the on and off rates intersect at 49.1 μM (i.e., K_d), which is nearly identical to the $K_{1/2}$, estimated from the dose–response relationship described above (Fig. 2 B). The agreement between this K_d value, obtained from kinetic parameters based on Scheme I, and the model-independent $K_{1/2}$ further demonstrates that Scheme I is adequate for describing glibenclamide block of K1250A-CFTR channels.

We then used the same method to obtain kinetic parameters for glibenclamide block at various membrane potentials. Visual inspections of the current traces shown in Fig. 3 A suggest that both open and blocked

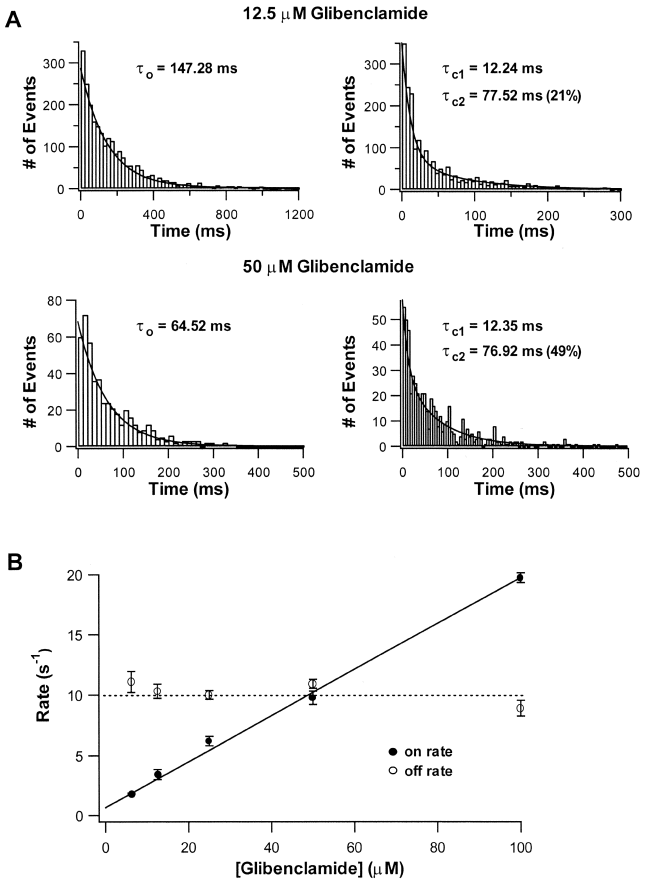

FIGURE 5. Relationships between kinetic parameters of glibenclamide block and glibenclamide concentration. (A) Open time (left) and closed time (right) histograms in the presence of 12.5 μM (top) or 50 μM glibenclamide (bottom). Open time histograms are fitted with a single exponential function (solid curve). Closed time histograms are fitted with a double exponential function (solid curve). The percentages of the slower component are 21% and 49% in the presence of 12.5 and 50 μM glibenclamide, respectively. (B) Relationships between the on (●) and off (○) rates of glibenclamide and glibenclamide concentrations. Solid line is a linear fit to the on rates. Dashed line is drawn by eyes to fit the off rates.

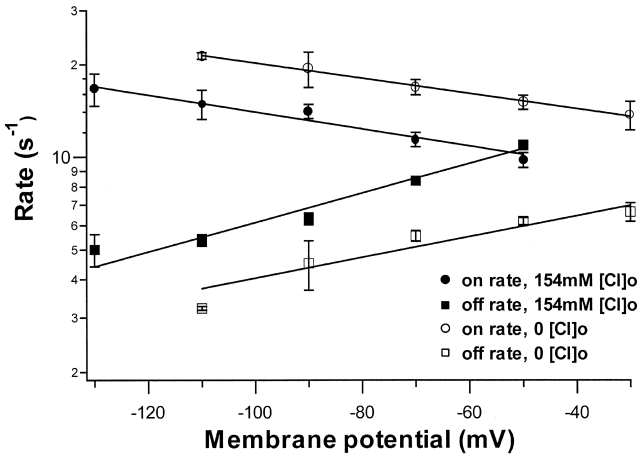

FIGURE 6. Voltage dependence of the on and off rates of glibenclamide block. Rates are extracted according to Scheme I. The on (●) and off rates (■) under symmetric Cl^- condition (154 mM $[Cl^-]o$/154 mM $[Cl^-]i$), and the on (○) and off rates (□) in the absence of external Cl^- (0 $[Cl^-]o$/154 mM $[Cl^-]i$) are plotted against the membrane potential. Solid lines are single exponential fits to the data. The differences between paired values (154 mM $[Cl^-]o$ versus 0 $[Cl^-]o$) at all voltages are statistically significant ($P < 0.05$) except the on rates at −110 mV ($P = 0.08$).

durations change with voltages. Membrane hyperpolarization increases both the number and duration of blocked events. Results from kinetic analysis indeed show that both k_{on} and k_{off} are voltage dependent (Fig. 6, filled symbols). Fitting the data in Fig. 6 with Eqs. 3 and 4 yields the values for δ_{on} of 0.16 ± 0.02 and δ_{off} of 0.28 ± 0.03 from inside of the channel. Thus, dissociation of glibenclamide seems somewhat more voltage dependent than association.

It has been shown that changing external $[Cl^-]$ affects the voltage dependence of blockers applied from inside (Linsdell and Hanrahan, 1996b; Linsdell et al., 1997; Sheppard and Robinson, 1997; Zhou et al., 2001b). We therefore examined the effect of extracellular $[Cl^-]$ on glibenclamide block. Fig. 7 A shows single-channel current traces in the presence of 50 μM glibenclamide with external Cl^- removed. Compared with glibenclamide block with 154 mM external Cl^- (Fig. 3 A), at any given membrane potential, channels stay in the open state shorter but in the blocked state longer. Thus, the Fb values in the absence of external Cl^- are higher than those in the presence of external Cl^- at all tested voltages (i.e., lower K_d at each voltage, Fig. 7 B). In addition, the slope of the voltage dependence curve is less steep (estimated $\delta_{Kd} = 0.32 \pm 0.05$) in the absence of external Cl^- than that in the presence of 154 mM external Cl^- (Fig. 7 B). Results from single-channel kinetic analysis indicate that both the on and off rates of glibenclamide block are sensitive to the presence of extracellular Cl^- (Fig. 6). In the absence of extracellular Cl^-, the on rates are larger at all voltages tested compared with those in the presence of 154 mM external Cl^-, whereas the off rates become smaller. Nevertheless, both the on and off rates are still voltage dependent (Fig. 6, open symbols). From the voltage dependence of k_{on} and k_{off}, the estimated electrical distances of glibenclamide measured from inside of the

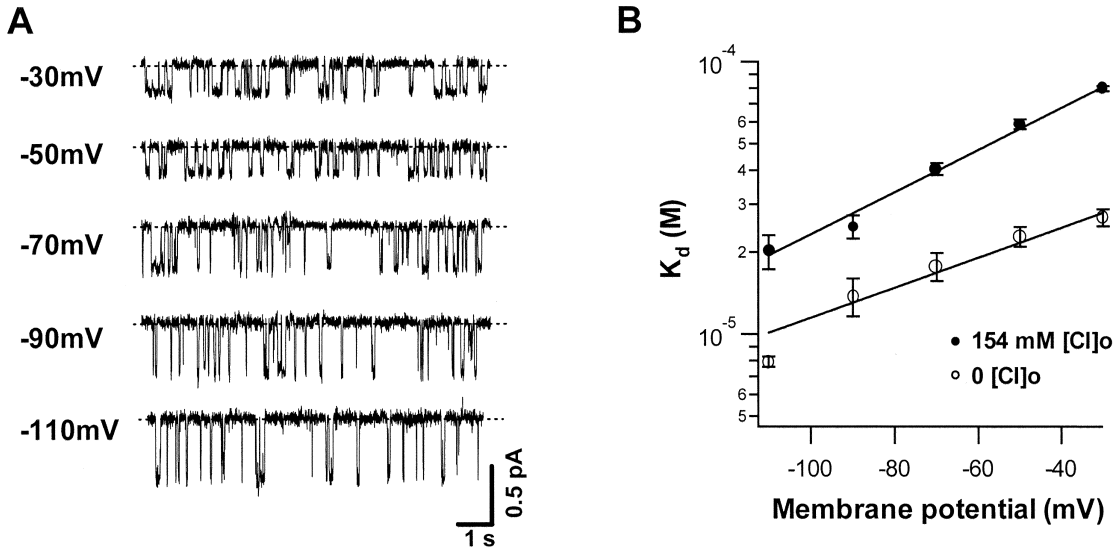

FIGURE 7. Voltage dependence of glibenclamide block in the absence of external Cl^-. (A) Single-channel current traces at various membrane potentials in the presence of 50 μM glibenclamide. (B) Voltage dependence of K_d in the absence of external Cl^- (○) and in the presence of 154 mM $[Cl^-]o$ (●). The differences between paired values at all voltages are statistically significant ($P < 0.05$) except at −110 mV ($P = 0.06$). Data are fitted with Eq. 5 (solid lines). $\delta_{Kd} = 0.45 \pm 0.03$ in the presence of 154 mM $[Cl^-]o$. $\delta_{Kd} = 0.32 \pm 0.05$ in the absence of external Cl^-.

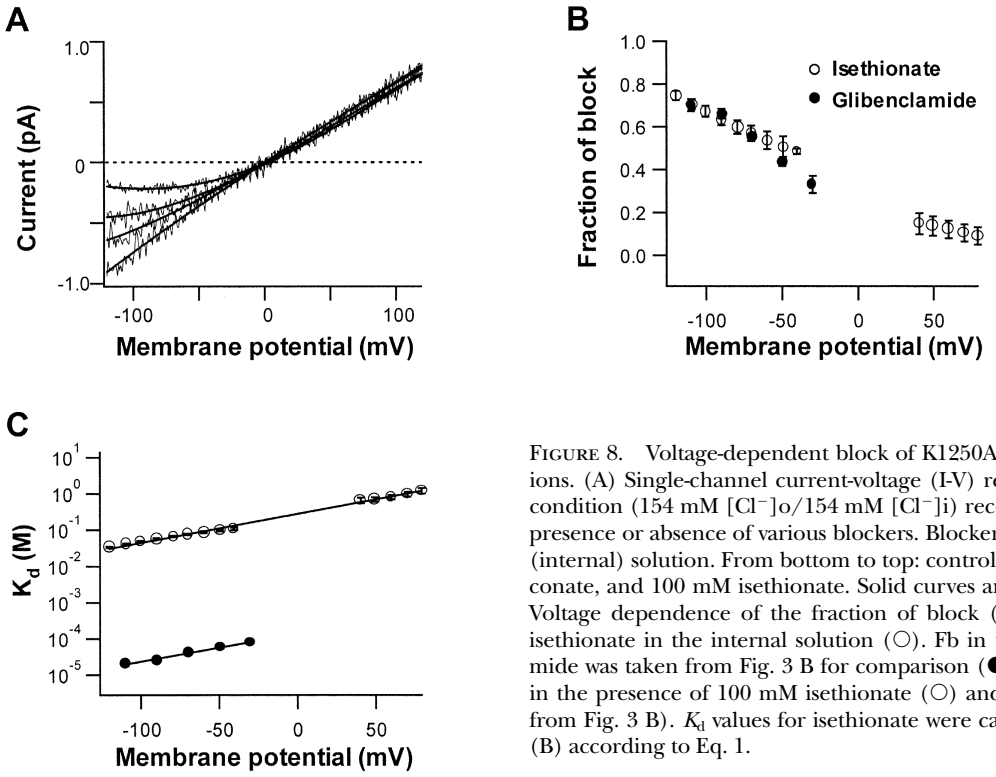

FIGURE 8. Voltage-dependent block of K1250A-CFTR by hydrophilic organic anions. (A) Single-channel current-voltage (I-V) relationships under symmetric Cl^- condition (154 mM $[Cl^-]o$/154 mM $[Cl^-]i$) recorded from the same patch in the presence or absence of various blockers. Blockers were applied to the superfusion (internal) solution. From bottom to top: control, 100 mM glutamate, 100 mM gluconate, and 100 mM isethionate. Solid curves are polynomial fits to the data. (B) Voltage dependence of the fraction of block (Fb) in the presence of 100 mM isethionate in the internal solution (○). Fb in the presence of 50 μM glibenclamide was taken from Fig. 3 B for comparison (●). (C) Voltage dependence of K_d in the presence of 100 mM isethionate (○) and 50 μM glibenclamide (●; taken from Fig. 3 B). K_d values for isethionate were calculated from Fb values shown in (B) according to Eq. 1.

pore in the absence of external Cl^- are 0.14 ± 0.01 (δ_{on}) and 0.19 ± 0.04 (δ_{off}), respectively.

Voltage-dependent Block of K1250A-CFTR Channels by Isethionate

Glibenclamide is a powerful tool to probe the CFTR pore because it affords direct measurements of both the on and off rate constants. However, this advantage is counteracted by the fact that a considerable single-channel signal-to-noise ratio is required for kinetic analysis. In addition, a fairly long duration of single-channel recording is necessary for collecting sufficient events. This latter requirement is especially problematic because membrane patches are unstable at relatively positive membrane potentials, precluding detailed quantification of glibenclamide block at positive voltages. We therefore set out to try several hydrophilic fast blockers to probe the CFTR pore.

We screened three large hydrophilic anions: gluconate, glutamate, and isethionate. Gluconate and glutamate are known CFTR channel blockers (Linsdell and Hanrahan, 1996b; Linsdell et al., 1997) and they block CFTR channels from intracellular side of the pore with a fast time scale. On the other hand, isethionate is used commonly as a replacement for Cl^- and there is no report so far that isethionate blocks CFTR channels. To our surprise, isethionate decreases the single-channel amplitude as if it also blocks the CFTR pore with a fast time scale (see below). To compare their ability to block K1250A-CFTR channels, we applied voltage ramps on inside-out patches in the presence or absence of various blockers in the perfusion solution. Fig. 8 A shows representative I-V curves of control and those in the presence of various blockers. All three anions block K1250A-CFTR channels in a voltage-dependent manner. However, at the same concentration (100 mM), isethionate shows the strongest block among these three anions. For example, at −100 mV, the values of Fb are 0.67 ± 0.01 (n = 7), 0.46 ± 0.02 (n = 7), and 0.33 ± 0.06 (n = 3) for isethionate, gluconate, and glutamate, respectively. Therefore, we focused on isethionate for the rest of the study. Fig. 8 B demonstrates that the voltage dependence of glibenclamide and isethionate block are very similar despite the very different time scales of action. Indeed, when the voltage-dependent K_d is quantified with Eq. 5, the electrical distance, δ_{Kd}, of isethionate block (0.45 ± 0.03) is identical to that of glibenclamide.

Fig. 9 A shows single-channel I-V curves in the presence of various concentrations of isethionate. The higher the concentration of isethionate, the smaller the single-channel amplitude. The values of Fb in the presence of different concentrations of isethionate were calculated as described above. The dose–response relationship, when fitted with the Michaelis-Menten function, yields a $K_{1/2}$ of 89.6 ± 3.4 mM at −50 mV (Fig. 9 B).

To test whether isethionate can also block the channel from the extracellular side, we applied isethionate

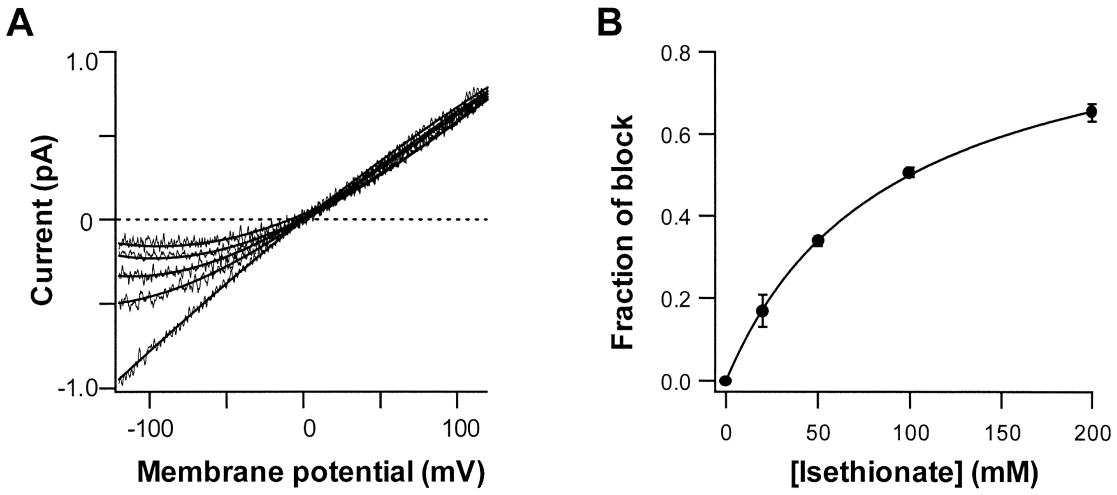

FIGURE 9. Dose–response relationship of internal isethionate block. (A) Single-channel current-voltage (I-V) relationships in the presence or absence of various amounts of isethionate under symmetric Cl^- condition (154 mM [Cl^-]o/154 mM [Cl^-]i). Isethionate was applied to the superfusion (internal) solution. From bottom to top: control, 20 mM isethionate, 50 mM isethionate, 100 mM isethionate and 200 mM isethionate. Solid lines are polynomial fits to the data. (B) Dose–response relationship of internal isethionate block. Fraction of block at −50 mV was obtained from I-V relationship. Solid line is the Michaelis-Menten fit to the data with a $K_{1/2}$ of 89.6 ± 3.4 mM (see Fig. 2 legend).

to the external solution in whole-cell recordings. Voltage-step protocols similar to those described above were performed (see Fig. 4) and representative current traces are shown in Fig. 10 A. In the presence of 76 mM isethionate in the external solution, the net whole-cell currents are similar to those of control. The steady-state I-V relationships in the absence or presence of external isethionate are nearly identical (Fig. 10 B), indicating that isethionate, at the tested concentration, has a negligible effect on CFTR current when applied from the external side of the channel.

Effect of Extracellular and Intracellular Cl^- on Isethionate Block

To investigate whether intracellular Cl^- affects isethionate block, we increased [Cl^-] in the bath solution to 300 mM (since it is technically difficult to maintain the excised patch at lower intracellular [Cl^-]) and tested isethionate block using the same ramp protocol described above. In the presence of 300 mM intracellular Cl^-, K_d values become larger compared with those in the presence of 154 mM intracellular Cl^- at all voltages tested (Fig. 11 A). δ_{Kd}, estimated from the voltage dependence of K_d in the presence of 300 mM intracellular Cl^-, is

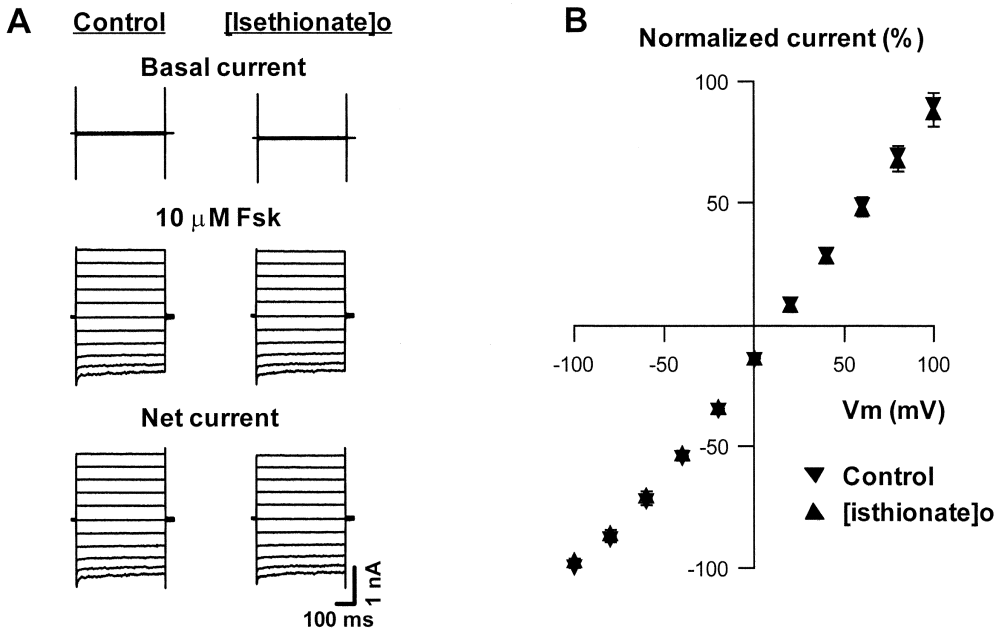

FIGURE 10. Effect of extracellular isethionate on K1250A-CFTR whole-cell current. (A) Whole-cell current response to voltage steps from −120 to 120 mV for 500 ms in 20-mV increments in the absence or presence of 76 mM external isethionate. K1250A-CFTR currents were activated by 10 μM Fsk. Net currents were obtained by subtracting the basal currents from that in the presence of 10 μM Fsk. (B) Steady-state current-voltage relationships in the absence (▼) or presence of 76 mM external isethionate (▲). Currents at different membrane potentials are normalized to that at −100 mV.

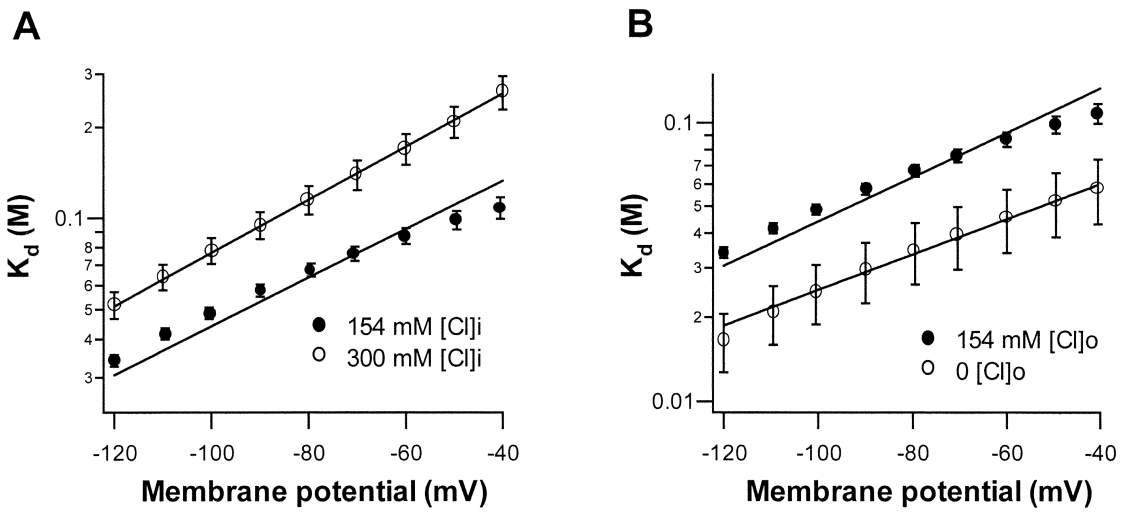

FIGURE 11. Effects of internal and external Cl^- concentrations on the voltage dependence of internal isethionate block. (A) Voltage dependence of K_d of isethionate block in the presence of 154 mM [Cl^-]i (●) or 300 mM [Cl^-]i (○). [Cl^-]o is 154 mM. The differences between paired values at all voltages are statistically significant ($P < 0.05$). K_d values are fitted with Eq. 5 (solid lines). $\delta_{Kd} = 0.45 \pm 0.03$ in the presence of 154 mM [Cl^-]i. $\delta_{Kd} = 0.50 \pm 0.01$ in the presence of 300 mM [Cl^-]i. (B) Voltage dependence of K_d of isethionate block in the presence of 154 mM [Cl^-]o (●) or 0 mM [Cl^-]o (○). [Cl^-]i is 154 mM. The differences between paired values at all voltages are statistically significant ($P < 0.05$). K_d values are fitted with Eq. 5. $\delta_{Kd} = 0.37 \pm 0.01$ in the absence of external Cl^-. $\delta_{Kd} = 0.45 \pm 0.03$ in the presence of 154 mM [Cl^-]o.

0.50 ± 0.01, which is similar to that in the presence of 154 mM intracellular Cl^- (Fig. 11 A). This result is consistent with the idea that intracellular Cl^- and isethionate may compete for the same binding site. When the concentration of competing Cl^- ions is increased, less block and a larger K_d are expected because of a lower probability of occupancy by isethionate at its binding site.

To test whether extracellular Cl^-, as in the case of glibenclamide block, affects isethionate block, we replaced Cl^- completely with aspartate in the pipette solution and examined isethionate block. In the absence of external Cl^-, isethionate block still shows voltage dependence and K_d values become smaller compared with those in the presence of 154 mM external Cl^- (Fig. 11 B). δ_{Kd}, estimated from the voltage dependence of K_d, is 0.37 ± 0.01, a value smaller than that in the presence of 154 mM external Cl^- (0.45 ± 0.03), but similar to the δ_{kd} (0.32 ± 0.05) for glibenclamide block in the absence of external Cl^- (Fig. 7 B). This result further supports the idea that glibenclamide and isethionate may share a common binding site.

Block of K1250A-CFTR by Mixture of Glibenclamide and Isethionate

If indeed these two blockers share a common binding site, then the kinetics of channel blockade by these two blockers can be described as:

$$XI \underset{k_1[I]}{\overset{k_{-1}}{\rightleftharpoons}} X \underset{k_{off}}{\overset{k_{on}'[G]}{\rightleftharpoons}} XG$$

SCHEME II

where X, XG, and XI represent the binding site, glibenclamide-occupied state and isethionate-occupied state, respectively. k_{on}' is the second-order rate constant for glibenclamide binding and k_{off} is the off rate of glibenclamide. k_{-1} is the off rate of isethionate and k_1 is the second-order rate constant for isethionate binding; [G] and [I] represent the concentrations of glibenclamide and isethionate respectively. According to Scheme II, the fractional block in the presence of both glibenclamide and isethionate (Fb_{G+I}) is given by:

$$Fb_{G+1} = \frac{K_{d(I)}[G] + K_{d(G)}[I]}{K_{d(I)}[G] + K_{d(G)}[I] + K_{d(G)}K_{d(I)}}, \quad (6)$$

where $K_{d(G)}$ and $K_{d(I)}$ are the dissociation constants of glibenclamide and isethionate, respectively. Since both $K_{d(G)}$ and $K_{d(I)}$ are known, we can calculate Fb_{G+I} at different combinations of glibenclamide and isethionate and experimentally verify the predictions. Fig. 12 A shows representative single-channel current traces and corresponding all-point amplitude histograms at –50 mV. In the presence of 6.25 μM glibenclamide plus 20 mM isethionate, both Po and single-channel amplitude decrease compared with those of control. When the concentrations of the blockers are increased, Po and single-channel amplitude further decrease. Fb_{G+I} was calculated as the ratio of the mean current, which takes into account both Po and the single-channel amplitude, in the presence of blockers and that in the absence of blockers. In all four different combinations of these two blockers, the experimentally measured Fb_{G+I} are in good agreement with the theoretical values

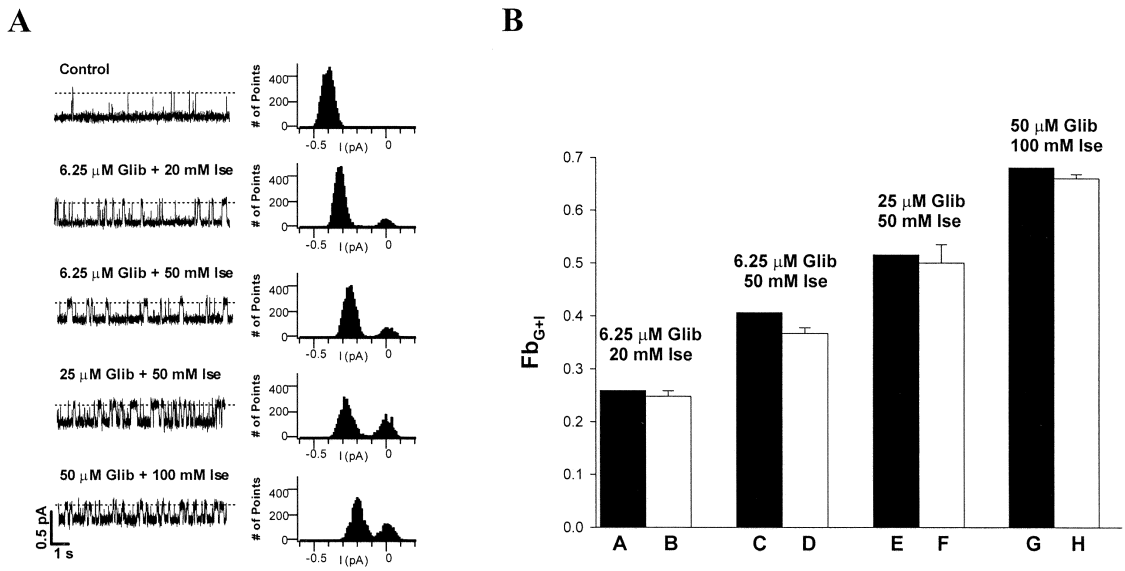

FIGURE 12. Block of K1250A-CFTR current in the presence of both glibenclamide and isethionate. (A) Single-channel current traces (left) and corresponding all-point amplitude histograms (right) in the absence (control) or presence of blockers, glibenclamide (Glib) and isethionate (Ise). Vm = −50 mV. (B) Fraction of block in the presence of Glib and Ise (Fb_{G+I}) with four different combinations of Glib and Ise. A, C, E, and G (black bars) are the predicted Fb_{G+I} values according to Scheme II and Eq. 6. B, D, F, and H (open bars) are experimental data.

based on Scheme II (Fig. 12 B). Scheme II also predicts that the apparent on rate of glibenclamide would decrease in the presence of isethionate since glibenclamide cannot bind when isethionate occupies the binding site, but the off rate would not be affected by isethionate. Since isethionate, being a fast blocker, reduces the single-channel amplitude and introduces extra open channel noise, we were only able to reliably perform our single-channel kinetic analysis at a low concentration of isethionate. Our results show that in the presence of 20 mM isethionate, the apparent on rate of glibenclamide (6.25 μM) is 1.38 ± 0.10 s^{-1} (n = 5), which is significantly slower than that in the presence of 6.25 μM glibenclamide alone (1.83 ± 0.06 s^{-1}, n = 4, see Fig. 5 B) ($P < 0.05$). In fact, this value of glibenclamide on rate in the presence of 20 mM isethionate is very close to the predicted value, 1.49 s^{-1}, based on Scheme II. On the other hand, the off rate of glibenclamide in the presence of isethionate is 10.97 ± 0.53 s^{-1} (n = 5), which is not different from that in the absence of isethionate (11.07 ± 0.86 s^{-1}, n = 4, see Fig. 5 B) ($P = 0.92$).

DISCUSSION

The goal of this study is to use the anion blockers, glibenclamide and isethionate, to probe the CFTR channel pore in order to understand the pore structure. We found that these two blockers, despite of their drastic differences in potency and blocking kinetics, show very similar voltage dependence and sensitivity to changes of external Cl^- concentration. Both anions block the CFTR channel from the cytoplasmic side of the membrane presumably traversing a significant distance into the pore to their binding site.

With the K1250A-CFTR mutant, we were able to quantify detailed kinetic parameters of glibenclamide block not provided by previous studies (Schultz et al., 1996; Sheppard and Robinson, 1997; Gupta and Linsdell, 2002). Our results demonstrate that both the on rate and the off rate of glibenclamide are voltage dependent (Fig. 6). In the presence of 154 mM external Cl^-, the electrical distance estimated from the on rate and the off rate are 0.16 and 0.28, respectively. The sum of these two values is close to the measured δ_{Kd} (δ_{Kd} = 0.45), as predicted (see MATERIALS AND METHODS). This latter value is similar to those derived from the voltage-dependent K_d reported previously for wt-CFTR (δ = 0.48, Sheppard and Robinson, 1997; δ = 0.41, Gupta and Linsdell, 2002). It should be noted that voltage-dependent blockade might not solely reflect the fact that the binding site of the blocker is in the electrical field. Studies of K^+ channels demonstrate that the voltage dependence of a blocker can be affected by the permeant ions entering the pore from the opposite side of the channel (e.g., Armstrong, 1971; Yellen, 1984; MacKinnon and Miller, 1988; Spassova and Lu, 1998). This trans-ion effect has also been shown in CFTR channels. External Cl^- concentration can affect the voltage-dependent block by glibenclamide (Sheppard and Robinson, 1997; Gupta and Linsdell, 2002), glutamate, and gluconate (Linsdell and Hanrahan, 1996b; Linsdell et al., 1997). We have also

reported that the voltage dependence of the intrinsic flickery blocking events seen in a locked-open K1250A-CFTR channel is mostly determined by the trans-ion effects (Zhou et al., 2001b). We tested the effect of external Cl^- on kinetic parameters of glibenclamide block. Our results show that the affinity of glibenclamide, as judged by K_d values, increases when external Cl^- is removed (Fig. 7 B). Detailed kinetic analysis show that the on rate of glibenclamide becomes faster and the off rate becomes slower in the absence of external Cl^- (Fig. 6). These observations suggest the presence of a Cl^- binding site external to the site for glibenclamide in the CFTR pore. Binding of Cl^- ions at this external site destabilizes glibenclamide binding.

It should be noted that Scheme I is the simplest model that is adequate to explain our results. We cannot rule out the possibility of other more complicated schemes. For example, the channel may be occupied by glibenclamide and the intrinsic blocker simultaneously. One would then expect three components in the closed time distribution. That the closed time distribution can be fitted quite well with a double exponential function (Fig. 5 A) suggests that if indeed the third component exists, it is not resolved under our experimental conditions. Unfortunately, the molecular nature of the intrinsic blocker remains a mystery. Future identification of the intrinsic blocker will permit differentiation of different kinetic schemes. Nevertheless, this limitation applied to glibenclamide blockade is not a concern for isethionate block because the block is assessed without a contamination of flickery block.

The voltage-dependent block of the CFTR pore is also seen with isethionate, a hydrophilic organic anion commonly used as a Cl^- substitute. Like other large hydrophilic anions, such as gluconate and glutamate (Linsdell and Hanrahan, 1996b; Linsdell et al., 1997), isethionate blocks CFTR channels in a voltage-dependent manner with a fast time scale. Surprisingly, isethionate is more potent than the two well-characterized blockers, gluconate and glutamate (Fig. 8 A). The K_d of isethionate at -100 mV is 48.7 mM compared with a K_d (-100 mV) of $\sim$80 mM for gluconate (Linsdell and Hanrahan, 1996b; Linsdell et al., 1997) and a K_d (-100 mV) of 325 mM for glutamate (Linsdell and Hanrahan, 1996b). Therefore, isethionate can be considered as a new tool to probe the CFTR pore.

Glibenclamide and isethionate block CFTR channels with different kinetics, and their binding affinities differ by three orders of magnitude. However, our results suggest that these two blockers may share a common binding site. First, the voltage dependence of glibenclamide block and isethionate block are nearly identical in the presence of 154 mM external Cl^- (Fig. 8, B and C). Second, in the absence of external Cl^-, the estimated δ_{Kd} values for both blockers are again very similar to each other, indicating that their voltage dependence is equally sensitive to changes of external Cl^- concentration. Third, when glibenclamide and isethionate are applied together (Fig. 12), the resulting Fb_{G+I} are compatible with the predicted values based on Scheme II that glibenclamide and isethionate compete for a common binding site. Although Scheme II seems reasonable, we cannot completely rule out the possibility that glibenclamide and isethionate may actually bind to two different sites that are very close to each other in the pore. Thus, both blockers can reside in the pore simultaneously. However, it seems difficult to envision that isethionate is able to enter a glibenclamide-occupied pore (and vice versa), since both blockers are fairly large in size. Furthermore, if indeed both blockers can bind at the same time while binding of one blocker does not affect binding of the other, the predicted Fb_{G+I} values will be higher than those predicted from Scheme II. Our experimental data are consistently closer to the values predicted from Scheme II, and are always smaller than those based on a model with two binding sites (unpublished data). Computational modeling based on the crystal structure, when available, would be able to differentiate between these two possibilities. Studies using mutants that affect glibenclamide and isethionate may also be useful.

If we accept the concept of one common binding site for both glibenclamide and isethionate, we are able to make some speculations about the CFTR pore based on the structural differences between these two blockers. Glibenclamide ($C_{23}H_{27}ClN_3O_5S^-$) is a large hydrophobic anion, whereas isethionate ($C_2H_5O_4S^-$) is a relatively small hydrophilic anion. The physical dimensions of both blockers are estimated using a program written by Dr. Xiaoqin Zou (University of Missouri). Briefly, the three-dimensional coordinates are generated by the CONCORD software (Rusinko et al., 1989) that determines the minimal and maximal coordinates that are occupied by a molecule along the x, y, and z axis, respectively. The molecular dimensions are then derived from these coordinates. The estimated dimensions of glibenclamide and isethionate are 21.4 Å $\times$ 13.6 Å $\times$ 11.6 Å and 8.1 Å $\times$ 5.8 Å $\times$ 6.2 Å, respectively. The slow on rate of glibenclamide (on the order of 10^5 $s^{-1}M^{-1}$) is probably due to its large size. Thus, a special orientation of glibenclamide may be required for the blocker to move across the internal entrance of the pore. The on rate of isethionate is likely to be faster than that of glibenclamide if we assume size is a main determinant of the on rate. Even if the on rate of both blockers are the same, the off rate of glibenclamide is at least a thousandfold slower than that of isethionate, since the K_d of glibenclamide is about three orders of magnitude smaller than that of isethionate. The slower off rate of glibenclamide suggests that glibenclamide

can bind much more stably to its binding site than isethionate. Since glibenclamide has three hydrophobic rings that are lacking in isethionate, we propose that there are likely to be some hydrophobic components in the pore that stabilize glibenclamide binding. Larger van der Waal's interactions between glibenclamide and the pore may also attribute to the tight binding. On the other hand, the negative charge of the blockers is also important, as indicated by previous research (Sheppard and Robinson, 1997). Therefore, positive charge as well as hydrophobic components in the pore are important for a stable binding of the blocker in the CFTR pore. It should be noted that this conclusion is valid irrespective of whether glibenclamide and isethionate bind to the same site or two nearby sites. Interestingly, based on studies with alkyl-TEA derivatives, Choi et al. (1993) made a similar conclusion on the pore structure of *Shaker* potassium channels. The presence of hydrophobic segment(s) in the aqueous pore is perhaps important to prevent CFTR channels from being blocked by hydrophilic anions (e.g., glutamate) present under physiological conditions in the cell.

In order for a blocker as large as glibenclamide to enter the pore from the cytoplasmic side, the internal entry of the pore should be at least ~11 Å wide, assuming the dimension of glibenclamide bound to the channel is similar to that measured from the crystal structure. In fact, the portion of the pore between the internal entrance and the blocker binding site should be as wide. Although the estimated electrical distance of glibenclamide block is only ~30% across the electrical field after eliminating the trans-ion effect, the actual physical distance glibenclamide travels into the pore is perhaps much larger because this predicted wide tunnel presents a low-resistance (i.e., smaller voltage drop) pathway for Cl^- ions as well as for water molecules. A similar discrepancy between electrical distance and physical distance has been described for the binding site of quaternary ammonium inhibitors in the pore of K^+ channels (Yellen et al., 1991; Zhou et al., 2001a). Therefore, instead of a wide internal vestibule for those sizable blockers to lodge (Linsdell and Hanrahan, 1996a; Zeltwanger et al., 2000), we propose a wide internal entrance followed by an at least equally wide tunnel that the blocker has to traverse before reaching its binding site.

On the other hand, the external entrance of the pore is likely to be narrower since blockers, such as disulphonic stilbenes (DNDS and DIDS), glutamate, gluconate, and isethionate can only block CFTR channels when applied intracellularly but not extracellularly (Gray et al., 1990; Tabcharani et al., 1990; Gadsby et al., 1995; Linsdell and Hanrahan, 1996a,b). Some other blockers, such as diphenylamine-2-carboxylate (DPC), flufenamic acid (FFA), and glibenclamide, are effective when applied to either side of the membrane. However, since these blockers are membrane permeant and it usually takes several minutes for them to exhibit a full blocking effect, it is likely that these blockers, even when applied extracellularly, actually block the channel from inside (Sheppard and Welsh, 1992; McCarty et al., 1993; Schultz et al., 1996; Sheppard and Robinson, 1997). Our results from single-channel recordings and whole-cell recordings indeed support the idea that glibenclamide, even applied extracellularly, enters the channel from the intracellular side of the pore. Only small permeant molecules, such as SCN^- and $Au(CN)_2^-$, have been observed to block the channel from either side of the membrane (Tabcharani et al., 1993; Mansoura et al., 1998; Smith et al., 1999; Gong et al., 2002; Linsdell and Gong, 2002; unpublished data). Together, CFTR channel pore may adopt an asymmetric structure with a relatively large internal tunnel and a fairly narrow external entrance. The existence of a stringent external entrance may provide some evolutionary advantages since CFTR is normally present in the apical membranes of intestinal epithelia and thus is exposed to a multitude of potential blockers.

The presence of a large internal tunnel allows us to make another structural prediction. Since the diameter of this internal tunnel has to be at least ~11 Å, whereas previous biophysical studies suggest a narrowest region (i.e., selectivity filter) of 6 Å in the CFTR pore (Linsdell and Hanrahan, 1996a), the selectivity filter should be located external to the glibenclamide/isethionate binding site because our data provide no evidence that glibenclamide or isethionate can pass through the channel. With the addition of this implied structural information, one can speculate that an open CFTR pore structure may show some resemblance to the recently resolved open-channel structure of the K^+ channels (Jiang et al., 2002).

Several of our results support the notion that CFTR channel has a pore that can be occupied simultaneously by multiple anions. First, effects of both blockers are sensitive to changes of external Cl^- concentration. Removing external Cl^- enhances both glibenclamide and isethionate block (Figs. 7 B and 11 B). Detailed kinetic analysis shows that the off rate of glibenclamide is faster in the presence of external Cl^- (Fig. 6). We reason that Cl^- ions can enter the pore from the external side to destabilize glibenclamide binding. Thus, the pore can be occupied by Cl^- and glibenclamide simultaneously and there is at least one Cl^- binding site external to the glibenclamide/isethionate binding site. This is also consistent with the picture described above that the selectivity filter (by definition a Cl^- binding site) is located external to the blocker

binding site. Second, the binding site for the blockers likely also binds Cl^- ions because increasing internal Cl^- concentration results in less block by isethionate (Fig. 11 A). Therefore, we conclude that at least two Cl^- binding sites are present in the CFTR pore. If these two binding sites are physically close to each other, a potential electrostatic repulsion between the two closely seated Cl^- ions can expedite Cl^- exit.

Channel's blockers have been used successfully to explore the pore structure of ion channels. While the crystal structure of CFTR channel is not yet available, blockers remain as powerful tools to study the CFTR pore. An important remaining question is where the gate of the CFTR channel is located along the anion-conducting pore. The slow kinetics of glibenclamide binding makes this blocker a good candidate to study the relationship between gating and blocking to gain more information about the structure of this intriguing molecule.

We thank Drs. Tsung-Yu Chen, Kevin Gillis and Allan Powe for critical reading of the manuscript, and Drs. Xiaoqin Zou and Olaf S. Andersen for helpful discussion.

This work is supported by the National Institutes of Health. Dr. Zhen Zhou is a recipient of a postdoctoral fellowship from the Cystic Fibrosis Foundation.

Submitted: 30 July 2002
Revised: 29 August 2002
Accepted: 24 September 2002

REFERENCES

Akabas, M.H., C. Kaufmann, T.A. Cook, and P. Archdeacon. 1994. Amino acid residues lining the chloride channel of the cystic fibrosis transmembrane conductance regulator. *J. Biol. Chem.* 269: 14865–14868.

Armstrong, C.M. 1971. Interaction of tetraethylammonium ion derivatives with the potassium channels of giant axons. *J. Gen. Physiol.* 58:413–437.

Choi, K.L., C. Mossman, J. Aube, and G. Yellen. 1993. The internal quaternary ammonium receptor site of Shaker potassium channels. *Neuron.* 10:533–541.

Cotton, J.F., and M.J. Welsh. 1999. Cystic fibrosis-associated mutations at arginine 347 alter the pore architecture of CFTR. Evidence for disruption of a salt bridge. *J. Biol. Chem.* 274:5429–5435.

Csanády, L. 2000. Rapid kinetic analysis of multichannel records by a simultaneous fit to all dwell-time histograms. *Biophys. J.* 78:785–799.

Doyle, D.A., J. Morais-Cabral, R.A. Pfuetzner, A. Kuo, J.M. Gulbis, S.L. Cohen, B.T. Chait, and R. MacKinnon. 1998. The structure of the potassium channel: molecular basis of K^+ conduction and selectivity. *Science.* 280:69–77.

Gadsby, D.C., G. Nagel, and T.-C. Hwang. 1995. The CFTR chloride channel of mammalian heart. *Annu. Rev. Physiol.* 57:387–416.

Gong, X., S.M. Burbridge, E.A. Cowley, and P. Linsdell. 2002. Molecular determinants of $Au(CN)_2^-$ binding and permeability within the cystic fibrosis transmembrane conductance regulator Cl^- channel pore. *J. Physiol.* 540:39–47.

Gray, M.A., C.E. Pollard, A. Harris, L. Coleman, J.R. Greenwell, and B.E. Argent. 1990. Anion selectivity and block of the small-conductance chloride channel on pancreatic duct cells. *Am. J. Physiol.* 259:C752–C761.

Gupta, J., and P. Linsdell. 2002. Point mutations in the pore region directly or indirectly affect glibenclamide block of the CFTR chloride channel. *Pflugers Arch.* 443:739–747.

Jiang, Y., A. Lee, J. Chen, M. Cadene, B.T. Chait, and R. MacKinnon. 2002. The open pore conformation of potassium channels. *Nature.* 417:523–526.

Jiang, Y., and R. MacKinnon. 2000. The barium site in a potassium channel by x-ray crystallography. *J. Gen. Physiol.* 115:269–272.

Linsdell, P. 2001. Thiocyanate as a probe of the cystic fibrosis transmembrane conductance regulator chloride channel pore. *Can. J. Physiol. Pharmacol.* 79:573–579.

Linsdell, P., and X. Gong. 2002. Multiple inhibitory effects of $Au(CN)_2^-$ ions on cystic fibrosis transmembrane conductance regulator Cl^- channel currents. *J. Physiol.* 540:29–38.

Linsdell, P., and J.W. Hanrahan. 1996a. Disulphonic stilbene block of cystic fibrosis transmembrane conductance regulator Cl^- channels expressed in a mammalian cell line and its regulation by a critical pore residue. *J. Physiol.* 496:687–693.

Linsdell, P., and J.W. Hanrahan. 1996b. Flickery block of single CFTR chloride channels by intracellular anions and osmolytes. *Am. J. Physiol.* 271:C628–C634.

Linsdell, P., J.A. Tabcharani, and J.W. Hanrahan. 1997. Multi-ion mechanism for ion permeation and block in the cystic fibrosis transmembrane conductance regulator chloride channel. *J. Gen. Physiol.* 110:365–377.

MacKinnon, R., and C. Miller. 1988. Mechanism of charybdotoxin block of the high-conductance, Ca^{2+}-activated K^+ channel. *J. Gen. Physiol.* 91:335–349.

Mansoura, M.K., S.S. Smith, A.D. Choi, N.W. Richards, T.V. Strong, M.L. Drumm, F.S. Collins, and D.C. Dawson. 1998. Cystic fibrosis transmembrane conductance regulator (CFTR) anion binding as a probe of the pore. *Biophys. J.* 74:1320–1332.

McCarty, N.A., S. McDonough, B.N. Cohen, J.R. Riordan, N. Davidson, and H.A. Lester. 1993. Voltage-dependent block of the cystic fibrosis transmembrane conductance regulator Cl^- channel by two closely related arylaminobenzoates. *J. Gen. Physiol.* 102:1–23.

McDonough, S., N. Davidson, H.A. Lester, and N.A. McCarty. 1994. Novel pore-lining residues in CFTR that govern permeation and open-channel block. *Neuron.* 13:623–634.

Miller, C. 1982. Bis-quaternary ammonium blockers as structural probes of the sarcoplasmic reticulum K^+ channel. *J. Gen. Physiol.* 79:869–891.

Riordan, J.R., J.M. Rommens, B.-S. Kerem, N. Alon, R. Rozmahel, Z. Grzelczak, J. Zielenski, S. Lok, N. Plavsic, J.-L. Chou, et al. 1989. Identification of the cystic fibrosis gene: Cloning and characterization of complementary DNA. *Science.* 245:1066–1072.

Rusinko, A., III, R.P. Sheridan, R. Nilakantan, K.S. Haraki, N. Bauman, and R. Venkataraghavan. 1989. Using CONCORD to construct a large database of three-dimensional coordinates from connection tables. *J. Chem. Inform. Comp. Sci.* 29:251–255.

Schultz, B.D., A.D. DeRoos, C.J. Venglarik, A.K. Singh, R.A. Frizzell, and R.J. Bridges. 1996. Glibenclamide blockade of CFTR chloride channels. *Am. J. Physiol.* 271:L192–L200.

Sheppard, D.N., and K.A. Robinson. 1997. Mechanism of glibenclamide inhibition of cystic fibrosis transmembrane conductance regulator Cl^- channels expressed in a murine cell line. *J. Physiol.* 503:333–346.

Sheppard, D.N., and M.J. Welsh. 1992. Effect of ATP-sensitive K^+ channel regulators on cystic fibrosis transmembrane conductance regulator chloride currents. *J. Gen. Physiol.* 100:573–591.

Sheppard, D.N., and M.J. Welsh. 1999. Structure and function of the CFTR chloride channel. *Physiol. Rev.* 79:S23–S45.

Smith, S.S., X. Liu, Z.R. Zhang, F. Sun, T.E. Kriewall, N.A. McCarty, and D.C. Dawson. 2001. CFTR: covalent and noncovalent modifi-

cation suggests a role for fixed charges in anion conduction. *J. Gen. Physiol.* 118:407–431.

Smith, S.S., E.D. Steinle, M.E. Meyerhoff, and D.C. Dawson. 1999. Cystic fibrosis transmembrane conductance regulator: Physical basis for lyotropic anion selectivity patterns. *J. Gen. Physiol.* 114: 799–818.

Spassova, M., and Z. Lu. 1998. Coupled ion movement underlies rectification in an inward-rectifier K^+ channel. *J. Gen. Physiol.* 112:211–221.

Tabcharani, J.A., W. Low, D. Elie, and J.W. Hanrahan. 1990. Low-conductance chloride channel activated by cAMP in the epithelial cell line T84. *FEBS Lett.* 270:157–164.

Tabcharani, J.A., J.M. Rommens, Y.-X. Hou, X.-B. Chang, L.-C. Tsui, J.R. Riordan, and J.W. Hanrahan. 1993. Multi-ion pore behavior in the CFTR chloride channel. *Nature.* 366:79–82.

Yellen, G. 1984. Relief of Na^+ block of Ca^{2+}-activated K^+ channels by external cations. *J. Gen. Physiol.* 84:187–199.

Yellen, G., M.E. Jurman, T. Abramson, and R. MacKinnon. 1991. Mutations affecting internal TEA blockade identify the probable pore-forming region of a K^+ channel. *Science.* 251:939–942.

Zeltwanger, S., F. Wang, G.T. Wang, K.D. Gillis, and T.-C. Hwang. 1999. Gating of cystic fibrosis transmembrane conductance regulator chloride channels by adenosine triphosphate hydrolysis. Quantitative analysis of a cyclic gating scheme. *J. Gen. Physiol.* 113:541–554.

Zeltwanger, S., Z.-R. Zhang, and N.A. McCarty. 2000. Glibenclamide inhibits CFTR activity through interaction with multiple sites with varying affinities and pH-dependences. *Biophys. ET J.* 78:A2752.

Zhou, M., J.H. Morals-Cabral, S. Mann, and R. MacKinnon. 2001a. Potassium channel receptor site for the inactivation gate and quaternary amine inhibitors. *Nature.* 411:657–661.

Zhou, Z., S. Hu, and T.-C. Hwang. 2001b. Voltage-dependent flickery block of an open cystic fibrosis transmembrane conductance regulator (CFTR) channel pore. *J. Physiol.* 532:435–448.